Opt Quant Electron (2017) 49:232
DOI 10.1007/s11082-017-1060-1

Revealing the target structure information encoded in strong-field photoelectron hologram

Mingrui He[1] · Yueming Zhou[1] · Yang Li[1] · Min Li[1] · Peixiang Lu[1,2]

Received: 8 April 2017 / Accepted: 18 May 2017 / Published online: 28 May 2017

Abstract By numerically solving the two-dimensional time-dependent Schrödinger equation, we investigate the strong-field photoelectron holography (SFPH) for different atomic and molecular targets. The results show that the photoelectron hologram is capable of providing structural information-the phase of scattering amplitude. In our calculations, the holographic pattern shifts with the target, indicating the phase difference between various targets. However, for the near-forward scattering, the phases of scattering amplitude for different targets are similar and thus no structural information has been retrieved in the previous works on near-forward scattering hologram. We suggest to use the backward scattering photoelectron hologram to extract this type of structural information. This paves a significant step towards time-resolved imaging of molecular structure and dynamics with the concept of SFPH.

Keywords Above-threshold ionization · Strong laser field · Ultrafast phenomena

✉ Yueming Zhou
zhouymhust@hust.edu.cn

Mingrui He
hmr_emma@hust.edu.cn

Yang Li
li_yang@hust.edu.cn

Min Li
mli@hust.edu.cn

[1] School of Physics, Huazhong University of Science and Technology, Wuhan 430074, People's Republic of China

[2] Laboratory of Optical Information Technology, Wuhan Institute of Technology, Wuhan 430205, People's Republic of China

1 Introduction

When an atom or molecule is exposed to a strong infrared laser field (Ke et al. 2017; Zhao et al. 2017), the target is first tunneling ionized with an electron wave packet (EWP) released. The ionized EWP is accelerated in the oscillating laser field and part of it can be driven back to revisit and scatter with the parent ion (Schafer 1993; Corkum 1993). During the rescattering process, various of electron-ion collision phenomena occur, such as high-order harmonic generation (HHG) (Krausz and Ivanov 2009; Mairesse 2003; Zhai 2016, 2017; Zhang 2017; Liu 2017), high-order above threshold ionization (Paulus 1994; Li 2015b, 2016; He 2016; Wang 2017; Li et al. 2017) and double ionization (Corkum 1993; Ma 2017; Zhou 2017; Huang et al. 2016). It has been shown that the released photons or rescattering EWPs encode the structural information of the atom or molecule (Lin 2010). Utilizing the rescattering process for self-imaging of the targets has been deeply investigated during the past years. For instance, using the HHG spectra, a tomographic reconstruction of the highest occupied molecular orbital of N_2 is accomplished (Itatani 2004). It has been theoretically predicted Morishita (2008) and experimentally confirmed (Okunishi 2008; Ray 2008) that the differential elastic scattering cross sections can be extracted from momentum distribution of the rescattered photoelectrons. Via controlling the recollision time of the returning EWP by changing the wavelength of the driving laser pulse, this experimental technique has been successfully extended to time-resolved imaging of ultrafast molecular dynamics (Blaga 2012).

Due to the coherent nature of the EWP in strong-field ionization, the rescattered electrons may interfere with the electrons that reach the detector directly after tunneling ionization. This type of interference is called strong field photoelectron holography (SFPH) (Huismans 2011), by analogy with the optical holography (Gabor 1948). Here, the rescattered wave packet acts as the signal wave and the direct wave packet acts as the reference wave. Because of the rescattering, structural information is encoded in the hologram. Recently, based on the adiabatic theory (Tolstikhin and Morishita 2012), we have explained that the structural information encoded in the hologram is the phase of scattering amplitude (Zhou et al. 2016). According to the quantum mechanism, scattering amplitude is a complex number determined by the magnitude and the phase. It is the full determination of scattering amplitude, both magnitude and phase, rather than the cross section that would provide complete meaningful information of the corresponding interaction. The exact determination of the phase of scattering amplitude is of great importance to many communities, ranging from chemistry, atomic physics to elementary particle physics. In previous studies on electron-atom/molecule collisions, usually only the cross section, which is the square modulus of the scattering amplitude, was extracted. While the phase of the scattering amplitude has been seldom measured. SFPH provides a feasible way to measure this type of structural information (Zhou et al. 2016). However, in previous experimental studies (Huismans 2011; Hickstein 2012; Meckel 2014), though the holographic interferences have been observed for various atomic and molecular targets, the difference in the interference patterns for different targets has not been revealed and thus no effort has been performed to extract the phase of the scattering amplitude. Here, by solving the two-dimensional time-dependent Schrödinger equation (TDSE) (Tong 2007), we investigate the SFPH originating from the near-forward rescattered and direct electrons. We find that the structural information-the phase of scattering amplitude of the target can be extracted from the photoelectron hologram. And the shift of holographic patterns for different targets reveals the phase difference between the targets.

However, the near-forward rescattering photoelectrons only have weak interaction with the targets. So that the near-forward scattering holographic patterns only provide limited structural information. It explains why the shifts of the holographic patterns are not prominent, and further, explains why there are no structural information retrieved from the near-forward scattering hologram in previous works. Our study will encourage further theoretical and experimental attempts on extracting phase of the scattering amplitude from backward scattering photoelectron hologram and provide a feasible method to self-image the structural information of the atoms and molecules using photoelectron holography.

2 Theory and results

The ionization of the targets are induced by mid-infrared few-cycle laser pulse that polarizes along z axis, with the wavelength of 1300-nm and pulse duration for 3 optical cycles (full width). The pulse envelope has a $\sin^2(\pi t/T_p)$ form. The laser intensity is chosen such that the Keldysh parameter (Keldysh 1965) $\gamma < 1$, i.e., in the tunneling regime. Here $\gamma = [I_p/(2U_p)]^{1/2}$, with $U_p = e^2F^2/(4m_e\omega^2)$ is the ponderomotive potential. F and ω are the amplitude and frequency of the laser field, respectively. I_p is the ionization potential of the target. For different targets, we alter the laser intensity to ensure the same Keldysh parameter $\gamma = 0.58$. Figure 1 illustrates the formation of SFPH. The EWP is first tunneling-ionized from the target and then oscillating in the laser field. Part of the EWP has no interaction with the ion core and reaches the detector directly. Another part is scattered near-forward by the core and thus records the ionic structure information. The interference

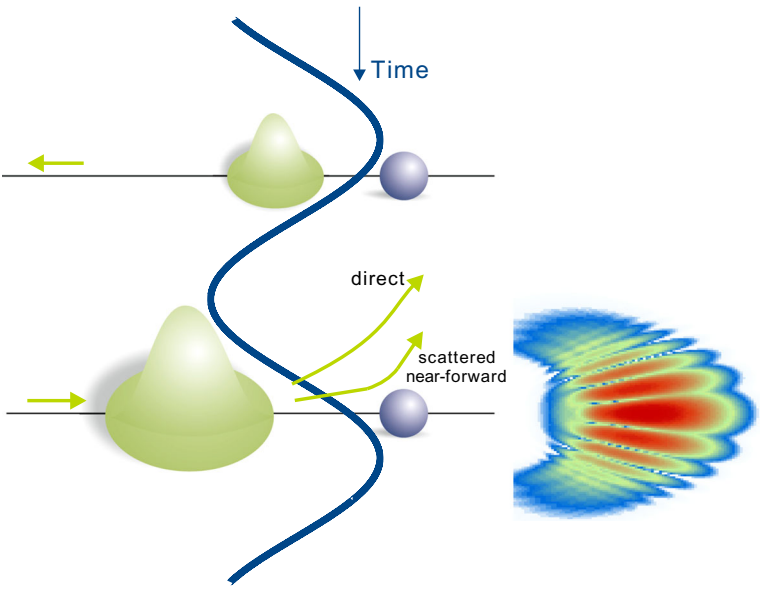

Fig. 1 Sketch of the formation of the photoelectron holography. During the interaction with the laser pulse (represented by *blue curve*), an EWP is firstly ionized, and then accelerated and finally driven back by the laser field. Part of the EWP recollides with parent ion and is scattered near-forward, interfering with the direct electrons. The SFPH pattern appears in the PEMD, manifests itself as fork-like interference fringes, as shown in the *right panel*

between the two parts of the EWP forms the fork-like near-forward holographic interference pattern in the photoelectron momentum distribution (PEMD), as depicted in the right panel of Fig. 1.

In the following, adopting the adiabatic theory (Tolstikhin and Morishita 2012), we briefly show how the phase of the scattering amplitude is encoded in SFPH. In the adiabatic theory, the ionization amplitude of the direct electron $\mathbf{I_d}(\mathbf{k})$ and rescattered electron $\mathbf{I_r}(\mathbf{k})$ are given by (atomic units are used throughout)

$$I_d(\mathbf{k}) = \mathbf{e}^{\mathbf{j}\pi/4}(2\pi)^{1/2}\sum_{\mathbf{i}}\frac{\mathbf{A_0}(\mathbf{k}_\perp,\mathbf{t_i})}{\sqrt{\mathbf{F}(\mathbf{t_i})}}\mathbf{e}^{[\mathbf{jS_d}(\mathbf{t_i},\mathbf{k})]}, \tag{1}$$

and

$$I_r(\mathbf{k}) = \mathbf{e}^{\mathbf{j}\pi/4}(2\pi)^{1/2}\sum_{\mathbf{i,r}}\frac{\mathbf{A_0}(\mathbf{u}_\perp(\mathbf{t_i}),\mathbf{t_i})}{\sqrt{(\mathbf{t_r}-\mathbf{t_i})\mathbf{F}(\mathbf{t_i})}\mathbf{f}(\mathbf{u}(\mathbf{t_r}),\theta)\mathbf{e}^{[\mathbf{jS_r}(\mathbf{t_i},\mathbf{t_r},\mathbf{k})]}}. \tag{2}$$

where

$$S_d(t_i,\mathbf{k}) = \frac{\mathbf{1}}{\mathbf{2}}\int_{-\infty}^{\mathbf{t_i}}[\mathbf{k}+\mathbf{v}(\mathbf{t})]^{\mathbf{2}}\mathbf{dt} - \mathbf{I_p}\mathbf{t_i}, \tag{3}$$

$$S_r(t_i,t_r,\mathbf{k}) = \frac{\mathbf{1}}{\mathbf{2}}\int_{-\infty}^{\mathbf{t_r}}[\mathbf{k}+\mathbf{v}(\mathbf{t})]^{\mathbf{2}}\mathbf{dt} - \frac{\mathbf{1}}{\mathbf{2}}\int_{\mathbf{t_i}}^{\mathbf{t_r}}\mathbf{u}(\mathbf{t})^{\mathbf{2}}\mathbf{dt} - \mathbf{I_p}\mathbf{t_i}. \tag{4}$$

In Eqs. (1–4), t_i and t_r are the ionization and recollision time, respectively. $\mathbf{F}(\mathbf{t})$ is the electric field and $\mathbf{v}(\mathbf{t}) = -\int_{-\infty}^{\mathbf{t}}\mathbf{F}(\tau)\mathbf{d}\tau$ is the vector potential. $\mathbf{k} = (\mathbf{k_z}, \mathbf{k}_\perp)$ is the final momentum while $\mathbf{u}(\mathbf{t_r})$ is incident momentum determined by $\mathbf{u}(\mathbf{t}) = \mathbf{v}(\mathbf{t}) - \frac{\mathbf{1}}{\mathbf{t_r}-\mathbf{t_i}}\int_{\mathbf{t_i}}^{\mathbf{t_r}}\mathbf{v}(\tau)\mathbf{d}\tau$. $A_0(k_\perp, t_i)$ is the amplitude of tunneling ionization with transverse momentum $k_\perp$ at the moment t_i (Batishchev et al. 2010). $f(\mathbf{u},\theta) = |\mathbf{f}(\mathbf{u},\theta)|\mathbf{e}^{\mathbf{j}\alpha(\mathbf{u},\theta)}$ is the elastic scattering amplitude for the scattering of free electrons by the target ion, where $\alpha(\mathbf{u},\theta)$ is the phase of the scattering amplitude with incident momentum $\mathbf{u}$ and scattering angle θ. The scattering angle is defined as $\theta = arctan(k_\perp/k_z)$.

With the ionization amplitude $\mathbf{I_d}(\mathbf{k})$ and $\mathbf{I_r}(\mathbf{k})$, the SFPH pattern in the final PEMD is

$$|\mathbf{I}(\mathbf{k})|^{\mathbf{2}} = |\mathbf{I_d}(\mathbf{k})|^{\mathbf{2}} + |\mathbf{I_r}(\mathbf{k})|^{\mathbf{2}} + \mathbf{2}|\mathbf{I_d}(\mathbf{k})||\mathbf{I_r}(\mathbf{k})|\cos(\triangle\phi), \tag{5}$$

where $\triangle\phi$ is the phase difference between the direct and rescattered EWPs. It can be written as

$$\triangle\phi \doteq \alpha + \frac{1}{2}k_\perp^2[t_r(0,k_z) - t_i(0,k_z)]. \tag{6}$$

The first term α on the right side of Eq. (6) is the phase of the scattering amplitude and the second term is determined by the laser field. When the laser field is known, t_i and t_r can be obtained by solving the corresponding saddle-point equations (Salières 2001), and thus the phase of the scattering amplitude could be extracted from the holographic pattern through Eq. (6). The details of this derivation was given in Lindner (2005) wherein the validity of Eq. (6) has been confirmed. Equation (6) also indicates that the phases of the scattering amplitudes for different targets are directly revealed by $\cos(\triangle\phi)$ when the driving laser pulses are the same. However, no study has been performed to reveal the shift of $\cos(\triangle\phi)$ for different targets. In the following, taking a further step on our previous study (Zhou

et al. 2016), we will show that the interference term $\cos(\triangle\phi)$ indeed changes with the target.

In our numerical calculation, the target ion is described by finite-range soft-core potential V(**r**). For atoms, $V(\mathbf{r}) = -e^{[-(\mathbf{r}/a)^2]}/\sqrt{\mathbf{r}^2 + b}$, and for diatomic molecules, $V(\mathbf{r}) = \sum_{\mathbf{i}=1,2} -\mathbf{e}^{[-(\mathbf{r}/\mathbf{a})^2]}/\sqrt{(\mathbf{r}-\mathbf{R_i})^2+\mathbf{b}}$, where $\mathbf{R_i}$ is the location of the i_{th} nuclei of the molecule. $a = 10$ is the Gaussian screening parameter that smoothly cuts off the infinite-range tail of the potential and b is the soft-core parameter. For He and Ne atoms, b are 1.62 and 2.28 a.u., respectively. For H_2^+, $b = 0.5$ a.u. Here we take H_2^+ aligned along the laser pulse polarization axis (z axis) with internuclear distance $R = 3.4$ a.u. as an example to demonstrate the extraction of the interference term $\cos(\triangle\phi)$ from SFPH pattern in PEMD.

The PEMD obtained by numerically solving TDSE (Tong 2007) is presented in Fig. 2a. The nearly horizontal fork-like interference structure is the near-forward SFPH (Huismans 2011) as described in Fig. 1. There also exist other types of interference such as the nearly vertical structure which originates from the intracycle interference of direct electrons (Lindner 2005; Arbó et al. 2006). To wash out this type of interference, we average the PEMD along the k_z direction. We choose a window function along the k_z direction with a width of 0.06 a.u. at an initial $k_z = k_i$. The value of k_i is the averaged value of PEMD within the window function. By scanning the k_z direction with the window function, the vertically distributed interference patterns can be washed out. The result is shown in Fig. 2b, where only holographic pattern is reserved in PEMD. Then we choose the slice at $k_z = U_p$ and the corresponding transverse momentum distribution is shown in Fig. 2c. Although the transverse momentum distribution curve has a Fraunhofer-like shape, the curve is believed to be the transverse momentum distribution of the near-forward scattering holographic pattern but not Fraunhofer-like diffraction demonstrated by Xin et al. (2015). Since for laser wavelength shorter than 2000 nm and internuclear distance smaller than 9 a.u., the Fraunhofer-like diffraction will be absent. According to Eq. (5), the modulation of this transverse momentum distribution results from the interference term $\cos(\triangle\phi)$, which

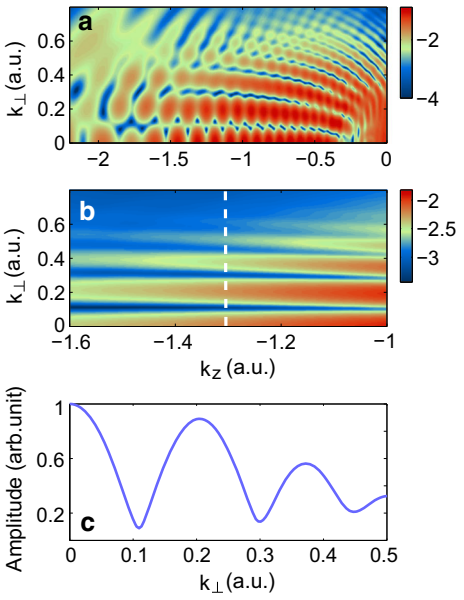

Fig. 2 **a** TDSE result of the PEMD of the H_2^+ aligned along polarization axis of the laser pulse with internuclear distance $R = 3.4$ a.u. ionized by the 1300-nm laser pulse. The intensity of the laser field is 2.3×10^{14}W/cm^2, for which the Keldysh parameter is 0.58. **b** Averaged PEMD obtained by averaging the spectrum in **a** with a square window function. **c** Transverse momentum distribution of the PEMD at the cut $k_\perp = U_p$ indicated by the white *dash line* in **b**

encodes the target structure information α through Eq. (6). In order to extract $\cos(\triangle\phi)$, we first subtract the envelope by assuming that the spectrum has the form

$$|I(k_\perp)|^2 = e^{\sigma(k_\perp)}[1 + g(k_\perp)\cos(\triangle\phi)]. \quad (7)$$

Here $e^{\sigma(k_\perp)}$ is the envelope of the extracted transverse momentum distribution. $\sigma(k_\perp)$ describes a monotonically decreasing background contribution, which is determined by fitting the logarithm of the averaged spectrum with the third-order polynomial. Dividing the spectrum from $e^{\sigma(k_\perp)}$, we get a smoother oscillating spectrum with the other envelope $g(k_\perp)$, which is again determined by performing the fitting procedure to the spectrum. Then the interference term $\cos(\triangle\phi)$ of the transverse momentum distribution is obtained, as presented by the blue line in Fig. 3a. We mention that the extraction of $\cos(\triangle\phi)$ does not depend on the type of functions we choose in fitting $e^{\sigma(k_\perp)}$ and $g(k_\perp)$.

So far, we have extracted the interference term $\cos(\triangle\phi)$ from SFPH. Via Eq. (6), the phase of the scattering amplitude could be easily retrieved. Here we will not retrieve the phase of the scattering amplitude, but compare the interference terms $\cos(\triangle\phi)$ for different targets to qualitatively show that phase difference of the scattering amplitudes for these targets is indeed expressed in SFPH. According to Eq. (6), the second term on the right side should be the same for different targets when ionization is induced by the the same laser pulse. Thus, the shift in $\cos(\triangle\phi)$ should directly indicate the different phases of scattering amplitudes for different targets.

To confirm that, we compare the $\cos(\triangle\phi)$ extracted from different targets with similar ionization potentials. Applying the above extraction procedure into the PEMD of He, whose ionization potential $I_p = 0.904$ a.u. is the same as that of H_2^+ at $R = 3.4$ a.u. We choose the same slice $k_z = U_p$. The ionization time t_i as well as the recollision time t_r is the same for both targets. So the extracted $\cos(\triangle\phi)$ for these two targets could directly reflect the difference between phases of scattering amplitudes. As shown in Fig. 3a, the shift between the two targets is very small.

For molecules, scattering amplitudes should be different for different orientations. In Fig. 3b, we compare $\cos(\triangle\phi)$ for H_2^+ aligned parallel (green line) and perpendicular (blue line) to the polarization axis of the laser pulse. The difference between two results is still

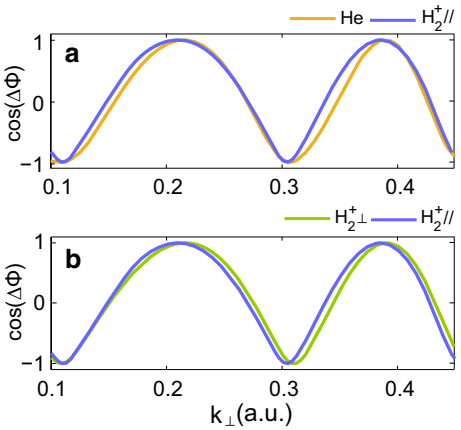

Fig. 3 **a** $\cos(\triangle\phi)$ extracted from the transverse momentum distribution for He (*orange line*) and H_2^+ aligned along the polarization axis with $R = 3.4$ a.u. (*blue line*). These two targets have the same ionization potential $I_p = 0.904$ a.u. **b** Same as **a** for H_2^+ aligned along the polarization axis (*blue line*) and H_2^+ aligned perpendicular to the polarization axis (*green line*). Other parameters are the same as Fig. 2. (Color figure online)

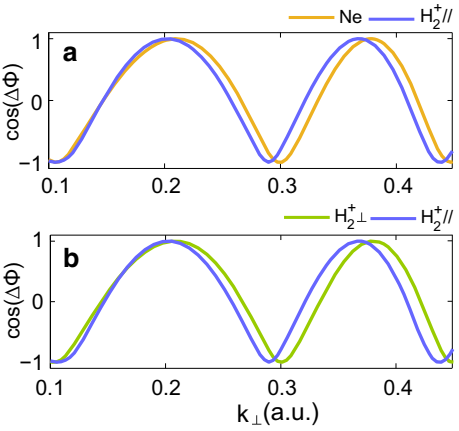

Fig. 4 Same as Fig. 3a, $\cos(\triangle\phi)$ for Ne atom (*orange line*) and H_2^+ aligned along the laser pulse polarization axis with $R = 4.6$ a.u. (*blue line*). The ionization potential $I_p = 0.79$ a.u. is the same for both targets. **b** for H_2^+ aligned parallel to polarization axis (*blue line*) and H_2^+ aligned perpendicular to the polarization axis (*green line*). The intensity of the laser field is 2.0×10^{14}W/cm^2, guaranteeing the Keldysh parameter $\gamma = 0.58$. (Color figure online)

very small. One should note that in the classical mechanism, the near-forward scattering (small scattering angles) corresponds to very large impact parameters and thus the near-forward rescattering SFPH only detects "out range" of the potential. For the molecule with small internuclear distance, the "out range" of the potentials are similar for parallel and perpendicular aligned molecules and corresponding atom. Thus, the shift in $\cos(\triangle\phi)$ between H_2^+ with different orientations and He is very small. Consequently, the holographic interferences are almost the same.

In Fig. 4, we present $\cos(\triangle\phi)$ extracted from another pair of targets, Ne and H_2^+ with $R = 4.6$ a.u. These two targets have the same ionization potential $I_p = 0.79$ a.u. Similar to Fig. 3, we compare the $\cos(\triangle\phi)$ for Ne and H_2^+ aligned along polarization axis in Fig. 4a. The shift between the results is more conspicuous than Fig. 3a. It is because that with the increasing internuclear distance, the structure of the molecule becomes more different from the corresponding atom. In Fig. 4b, we compare the extracted $\cos(\triangle\phi)$ for H_2^+ aligned parallel and perpendicular to the polarization axis. The shift between the two results is more obvious than the case with smaller internuclear distance in Fig. 3b as well.

From Figs. 3b and 4b, we find that for larger internuclear distance, the difference between $\cos(\triangle\phi)$ is more obvious. To confirm that, we investigate the H_2^+ with different internuclear distance R. Figure 5a–d correspond to R from 3 to 6 a.u. When R is small, the difference in the phases of the scattering amplitudes of the parallel and perpendicular aligned molecules is very small. So the shift of the holographic interference fringes between the two cases is small. As R increases, the phase difference of the scattering amplitudes for different alignments becomes larger and thus the shift of interference fringes in the hologram becomes visible, as shown in Fig. 5. Our numerical results confirm that the difference in the phases of the scattering amplitudes could be recorded by the photoelectron hologram and thus SFPH is capable of measuring the phase of the scattering amplitude.

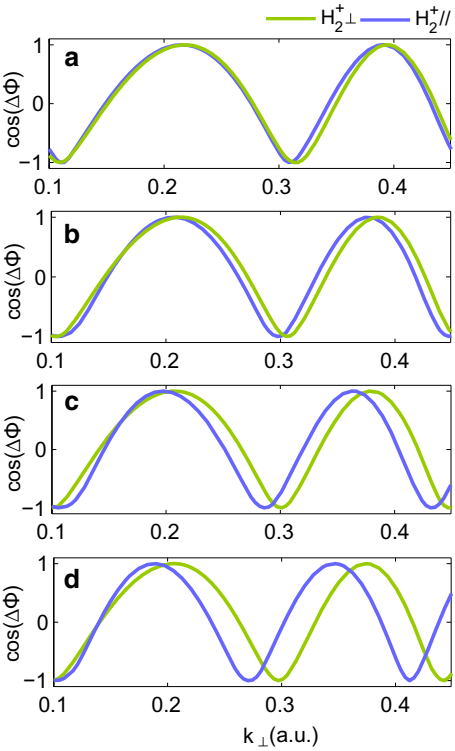

Fig. 5 $\cos(\triangle\phi)$ extracted from the transverse momentum distribution of H_2^+ with different internuclear distance R. **a–d** correspond to $R = 3, 4, 5$ and 6 a.u. In the four panels, the *blue lines* are H_2^+ with parallel orientation, while the *green lines* are H_2^+ with perpendicular orientation. The laser intensity was chosen to keep the Keldysh parameter is 0.58 for the all of the four panels. (Color figure online)

3 Conclusion

In summary, we have studied SFPH by numerically solving TDSE. Our results show that the holographic interference is indeed shifted for different targets, which directly indicates the structural information-the phase of the scattering amplitude. For the near-forward scattering holography, the rescattered electron only encodes the out range of the potential, which is similar for the usual atomic and small molecular targets, and thus the holographic patterns are almost the same for different atoms and molecules with small internuclear distance. This explains why previous experiments on SFPH for different targets have not observed any difference in the photoelectron holograms. In order to get information deep inside the potential of the targets, one needs to detect the holography between the backward rescattered and direct electrons. Thus, near-backward rescattering photoelectron holography will be a very important tool to probe the structural information (Bian and Bandrauk 2012; Li 2015a; Haertelt 2016). Because the SFPH also stores the temporal information about the core and electron dynamics, near-backward scattering SFPH will be an exciting prospect in time-resolved imaging of the ultrafast dynamics.

Acknowledgements This work was supported by the National Natural Science Foundation of China under Grant Nos. 61405064, 11234004, 11604108 and 61475055. Numerical simulations presented in this paper were carried out using the High Performance Computing Center experimental testbed in SCTS/CGCL.

References

Arbó, D.G., Persson, E., Burgdörfer, J.: Time double-slit interferences in strong-field tunneling ionization. Phys. Rev. A **74**, 063407 (2006)

Batishchev, P.A., Tolstikhin, O.I., Morishita, T.: Atomic Siegert states in an electric field: transverse momentum distribution of the ionized electrons. Phys. Rev. A **82**, 023416 (2010)

Bian, X.B., Bandrauk, A.D.: Attosecond time-resolved imaging of molecular structure by photoelectron holography. Phys. Rev. Lett. **108**, 263003 (2012)

Blaga, C., et al.: Imaging ultrafast molecular dynamics with laser-induced electron diffraction. Nature **483**, 194–197 (2012)

Corkum, P.B.: Plasma perspective on strong-field multiphoton ionization. Phys. Rev. Lett. **71**, 1994 (1993)

Gabor, D.: A new microscopic principle. Nature (London) **161**, 777–778 (1948)

Haertelt, M., et al.: Probing molecular dynamics by laser-induced backscattering holography. Phys. Rev. Lett. **116**, 133001 (2016)

He, M., et al.: Temporal and spatial manipulation of the recolliding wave packet in strong-field photoelectron holography. Phys. Rev. A **93**, 033406 (2016)

Hickstein, D., et al.: Direct visualization of laser-driven electron multiple scattering and tunneling distance in strong-field ionization. Phys. Rev. Lett. **109**, 073004 (2012)

Huang, C., et al.: Role of Coulomb repulsion in correlated-electron emission from a doubly excited state in nonsequential double ionization of molecules. Phys. Rev. A **93**, 013416 (2016)

Huismans, Y., et al.: Time-resolved holography with photoelectrons. Science **331**, 61–64 (2011)

Itatani, J., et al.: Tomographic imaging of molecular orbitals. Nature **432**, 867–871 (2004)

Ke, S., Wang, B., Long, H., Wang, K., Lu, P.: Topological mode switching in a graphene doublet with exceptional points. Opt Quant Electron. **49**(6) (2017). doi:10.1007/s11082-017-1054-z

Keldysh, L.V.: Ionization in the field of a strong electromagnetic wave. Sov. Phys. JETP **20**, 1307–1314 (1965)

Krausz, F., Ivanov, M.: Attosecond physics. Rev. Mod. Phys. **81**, 163–234 (2009)

Li, M., et al.: Revealing backward rescattering photoelectron interference of molecules in strong infrared laser fields. Sci. Rep. **5**, 8519 (2015). doi:10.1038/srep08519

Li, Y., et al.: Nonadiabatic tunnel ionization in strong circularly polarized laser fields: counterintuitive angular shifts in the photoelectron momentum distribution. Opt. Express **23**, 28801–28807 (2015)

Li, Y., et al.: Identifying backward-rescattering photoelectron hologram with orthogonal two-color laser fields. Opt. Express **24**, 23697–23706 (2016)

Li, Y., Li, M., Zhou, Y., Ma, X., Xie, H., Lan, P., Lu, P.: Carrier-envelope phase dependent photoelectron energy spectra in low intensity regime. Opt Express **25**(10), 11233–11243 (2017)

Lin, C.D., et al.: Strong-field rescattering physics—self-imaging of a molecule by its own electrons. J. Phys. B **43**, 122001 (2010)

Lindner, F., et al.: Attosecond double-slit experiment. Phys. Rev. Lett. **95**, 040401 (2005)

Liu, X., et al.: Probing the $\pi - \pi*$ transitions in conjugated compounds with an infrared femtosecond laser. Phys. Rev. A **95**, 033421 (2017)

Ma, X., et al.: Nonsequential double ionization of Xe by mid-infrared laser pulses. Opt. Quant. Electron. **49**, 170 (2017). doi:10.1007/s11082-017-1002-y

Meckel, M., et al.: R. Dörner, and M. Spanner, Signatures of the continuum electron phase in molecular strong-field photoelectron holography. Nat. Phys. **10**, 594–600 (2014)

Mairesse, Y., et al.: Attosecond synchronization of high-harmonic soft X-rays. Science **302**, 1540–1543 (2003)

Morishita, T., et al.: Accurate retrieval of structural information from laser-induced photoelectron and high-order harmonic spectra by few-cycle laser pulses. Phys. Rev. Lett. **100**, 013903 (2008)

Okunishi, M., et al.: Experimental retrieval of target structure information from laser-induced rescattered photoelectron momentum distributions. Phys. Rev. Lett. **100**, 143001 (2008)

Paulus, G.G., et al.: Rescattering effects in above-threshold ionization: a classical model. J. Phys. B **27**, L703 (1994)

Ray, D., et al.: Large-angle electron diffraction structure in laser-induced rescattering from rare gases. Phys. Rev. Lett. **100**, 143002 (2008)

Salières, P., et al.: A. Sanpera, and M. Lewenstein, Feynman's path-integral approach for intense-laser-atom interactions. Science **292**, 902–905 (2001)

Schafer, K.J., et al.: Above threshold ionization beyond the high harmonic cutoff. Phys. Rev. Lett. **70**, 1599–1602 (1993)

Tolstikhin, O.I., Morishita, T.: Adiabatic theory of ionization by intense laser pulses: finite-range potentials. Phys. Rev. A **86**, 043417 (2012)

Tong, X., et al.: Numerical observation of the rescattering wave packet in laser-atom Interactions. Phys. Rev. Lett. **99**, 093001 (2007)
Wang, Z., et al.: Correlated electron-nuclear dynamics in above-threshold multiphoton ionization of asymmetric molecule. Sci. Rep. **7**, 42585 (2017)
Xin, L., et al.: Fraunhofer-like diffracted lateral photoelectron momentum distributions of H_2^+ in charge-resonance-enhanced ionization in strong laser fields. Phys. Rev. A **92**, 063803 (2015)
Zhai, C., et al.: Coulomb-corrected molecular orbital tomography of nitrogen. Sci. Rep. **6**, 23236 (2016)
Zhai, C., et al.: Diffractive molecular-orbital tomography. Phys. Rev. A **95**, 033420 (2017)
Zhao, D., Wang Z-Q., Long H., Wang K., Wang B., Lu, P.-X.: Optical bistability in defective photonic multilayers doped by graphene. Opt Quant Electron. **49**(4) (2017). doi:10.1007/s11082-017-0999-2
Zhang, X., et al.: Ellipticity-tunable attosecond XUV pulse generation with a rotating bichromatic circularly polarized laser field. Opt. Lett. **42**, 1027–1030 (2017)
Zhou, Y., et al.: Near-forward rescattering photoelectron holography instrong-field ionization: extraction of the phase of the scattering. Opt. Express **25**, 8450–8458 (2017)
Zhou, Y., Tolstikhin, O.I., Morishita, T.: Near-forward rescattering photoelectron holography instrong-field ionization: extraction of the phase of the scattering. Phys. Rev. Lett. **116**, 173001 (2016)